Privacy Preserving Strong Simulation Queries on Large Graphs

Lyu Xu[1] Jiaxin Jiang[1] Byron Choi[1] Jianliang Xu[1] Sourav S Bhowmick[2]
[1]Department of Computer Science
Hong Kong Baptist University, Hong Kong
{cslyuxu, jxjian, bchoi, xujl}@comp.hkbu.edu.hk
[2]School of Computer Science and Engineering
Nanyang Technological University, Singapore
assourav@ntu.edu.sg

***Abstract*—This paper studies privacy preserving query services for strong simulation queries in the database outsourcing paradigm. In such a paradigm, clients send their queries to a third-party service provider (*SP*), who has the outsourced large graph data, and the *SP* computes the query answers. However, as *SP* may not always be trusted, the sensitive information of the clients' queries, importantly, the query structures, should be protected. Moreover, graph pattern queries often have high complexities, whereas data graphs can be large. This paper adopts *strong simulation* as a practical query semantic for this paradigm. Under this semantic, queries are matched with a notion of *balls*, which are subgraphs related to the query diameter. We transform the core of the existing strong simulation algorithm using *data-oblivious* operations (*ObSSA*) and propose its secure version. We show that the algorithm may encounter an overflow problem even partially homomorphic encryption (*PHE*) has been used. We then propose an efficient inexact algorithm *EncSSA*, which is secure under chosen plaintext attack (*CPA*). The results of privacy analysis are presented. We have conducted experiments on Twitter and Citeseer datasets, and the results show that *EncSSA* is both efficient and effective.**

***Index Terms*—Graph queries, strong simulation, large graphs, data outsourcing, privacy preservation**

I. Introduction

Graph pattern queries are increasingly found in emerging applications, including social networks, biology analysis, and communication networks [1]–[3]. However, some query formalisms are computationally costly, for example, the *subgraph isomorphism query* (*sub-iso*) is an *NP-complete* problem [4]. *Subgraph homomorphism*, used in the *SPARQL query on the RDF data* [5] with the same definition as *sub-iso* except that *sub-iso* has a bijective restriction on the matching, whereas *homomorphism* has an injective restriction [6]. These queries, however, can be too restricted for some applications. *Graph simulation query* [7] has been proposed, which can be computed in quadratic time but only support topology constraints on the children of each vertex. Similarly, *dual simulation query* [8], [9] preserves topological constraints on *both* the children and parents. *Strong simulation query* [9] has been then proposed to *strike a balance* between computation complexity and the capability to capture topological constraints.

In social search, strong simulation queries can be used to find an entity with specific types of connections or attributes. In recommender systems, such queries help individuals form collaboration networks with people having specific skills [9]–[11]. However, queries can be sensitive, as described below.

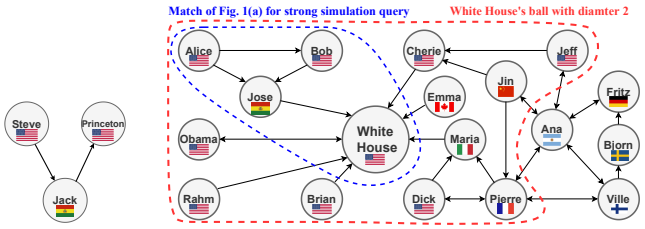

(a) User pattern (b) A small subset of Twitter

Fig. 1: A strong simulation query on a simplified Twitter[1] (Flags are labels. Text is for discussions but not queried.)

Example 1. *(Privacy preserving query processing in data outsourcing) Take the social network* Twitter *as an example, where vertices are (virtual) entities, labels are nationalities, and edges are interactions. Fig. 1(a) is a user pattern of user* Jack. Jack *finds whether there exist similar labeled patterns in* Twitter. *In this scenario, outsourcing the searches to an SP has a number of advantages, including elasticity, high availability and cost savings, when compared to on-premise solutions. However, SP may not always be trusted.* Jack *does not want to expose the interactions of nationalities (flags) he searches (i.e., to protect his query structure) from the SP. Similar scenarios can be found, e.g., in collaboration networks.* □

Matching queries on the data graph at a large scale, especially with privacy preservation, is challenging. This paper adopts strong simulation as the query semantic because the queries are evaluated on the *balls* of the graph [9], which are the subgraphs being defined by their centers and radius (see details in Sec. II). Our experiments on benchmarked queries and real datasets show that balls contain several hundred vertices (Tab. IV). This opens up an opportunity for private query processing at the *SP*. Consider Example 1 and take "*White House*" as the ball center with a radius 2. Strong simulation searches the pattern in Fig. 1(a) within the ball of "*White House*" in Fig. 1(b), where privacy preserving computation is achievable in a ciphertext domain. In this paper, we investigate privacy preserving *strong simulation query*.

There have been a variety of research works on querying with privacy preservation in graph databases (see Sec. VII for details). To the best of our knowledge, strong simulation query that protects the structure information of the query in the data

[1]D. Andrew, and V. Bertacco. "Electronic design automation for social networks." Proceedings of the 47th Design Automation Conference. 2010.

outsourcing paradigm has not been studied yet. This problem has the following two main technical challenges.

1) First, how to design an algorithm for strong simulation queries using *data-oblivious computation* [12] consisting of *data access patterns* that do not depend on the input?
2) Second, how to design algorithms that strike the balance between efficiency and privacy?

For the first challenge, our idea is to represent the query and each ball in the data graph using the adjacency matrix. Then, we replace the strong simulation algorithm with a *series of matrix operations*, which are data-oblivious. We propose an *ObSSA* algorithm based on the state-of-the-art [9] with only these operations. Given a query, *ObSSA* must carry out the same operations for each element in the result matrix *iteratively* until a fixed point, where the number of iterations is bounded by the ball size.

To tackle the second challenge, we derive an encoding and adopt an encryption for the matrices. Fully homomorphic encryption (*FHE*) [13] cannot be adopted due to its known poor performance. Most of the existing partially homomorphic encryption (*PHE*) schemes (e.g., EIGamal, Paillier and Boneh-Goh-Missm) [14], [15] cannot support *both* additions and multiplications simultaneously more than once, which are needed by *ObSSA*. We adopt the encryption method, namely *cyclic group based encryption scheme (CGBE)*, which is proposed by Fan et al. [16]. *CGBE* supports both the additions and multiplications simultaneously but does not allow the plaintext value of each ciphertext exceeding a *public value*. Using *CGBE*, we propose an encrypted version of *ObSSA*.

There is a further technical challenge from the encrypted *ObSSA*. Checking the definition of strong simulation requires multiple iterations that involve multiplications. Consequently, there will be an *overflow* in the computed ciphertext that the corresponding plaintext is larger than the given public value, *e.g.*, a prime with 2048 bits used in [16].

To strike the balance between privacy and a practical algorithm, we propose an inexact algorithm *EncSSA* that consists of three efficient optimizations. (The inexact algorithm can have false positives but no false negatives.) The first idea is to exploit localized algorithms for 2-hop neighbors so that the encryption algorithm does not encounter ciphertext overflow. The second idea is to check strong simulation using a subset of possible paths derived from the query's labels with a length k larger than 2. The last idea is to check the set of labels of h-hop neighbors where h is larger than k. These optimizations avoid excessive multiplications in the ciphertext domain, prune true negatives of the query results and achieve good efficiency.

Contributions. The contributions of this paper are as follows.

- We proposed the *ObSSA* algorithm to answer the strong simulation query under the plaintext setting, which transforms the key operations of the existing strong simulation algorithm with only data-oblivious mathematical operations.
- Based on the *CGBE* encryption scheme, we propose a practical and secure inexact algorithm *EncSSA* that comprises three privacy preserving pruning techniques.
- We present privacy analysis results of our proposed *EncSSA*.
- Our experiments verified the performance of *EncSSA*.

Organization. The preliminaries and the problem statement are introduced in Sec. II. We present the *ObSSA* algorithm in Sec. III and then the *EncSSA* algorithm in Sec. IV. The privacy analysis results are presented in Sec. V. Sec. VI presents the experimental results and Sec. VII discusses the recent related work. We conclude this paper with future work in Sec. VIII.

II. Preliminaries and Problem Formulation

In this section, we first provide preliminaries related to strong simulation and system models for technical discussions. It then presents the problem statement of the paper.

A. Graph Data and Pattern Query Semantics

Graph. A *graph* is denoted by $G = (V_G, E_G, \Sigma_G, L_G)$, where V_G, E_G, Σ_G, L_G are the sets of vertices, directed edges, labels and the function for matching the vertices with their labels. (u,v) denotes the directed edge from vertex u to v and $L_G(u)$ denotes the label value of u. For a connected graph G, the *distance* between any two vertices u and v in G, denoted by $\mathsf{dis}(u,v)$, is the length of the shortest undirected paths from u to v in G while the *diameter* of G, denoted by d_G, is the largest shortest distance between all pairs of vertices in G.

Ball. A *ball* $B = (V_B, E_B, \Sigma_B, L_B, u, r)$, denoted by $G[u, r]$, is a connected subgraph of G which takes vertex u as *center*, r as *radius*, such that, (a) $V_B = \{v | v \in V_G, \mathsf{dis}(u, v) \leq r\}$, and (b) E_B has the edges that appear in G over the same vertices in V_B [9]. The size of ball, $|V_B|$, is restricted by r. The strong simulation query searches for matches within balls, as opposed to the whole data graph.

Adjacency matrix. The *adjacency matrix* of graph G, denoted by M_G, is a $|V_G|\times|V_G|$ matrix. M_G's transport matrix is denoted by M_G^{T}. The i^{th} row vector of M_G is denoted by $M_G(i)$ and the j^{th} element in $M_G(i)$ is denoted by $M_G(i,j)$.

We remove the subscript G when it is clear from the context. To make the definition of query semantic consistent with this paper's notations, we introduce the *vertex mapping matrix* and rewrite the definition of strong simulation query.

Vertex mapping matrix. The *vertex mapping matrix* from a query Q to a graph G, denoted by P, is a $|V_Q|\times|V_G|$ matrix. $P(i,j)$=1 if $L_Q(v_i)$=$L_G(v_j)$, $v_i \in V_Q$ and $v_j \in V_G$. Otherwise, $P(i,j)$=0. The i^{th} row vector of P is denoted by $P(i)$.

The vertex mapping matrix uses a 1 (a possible mapping) to denote that a vertex of the query and a vertex of the graph have the same label, and 0 otherwise. For any vertex u in Q, if vertex v in G satisfies $L_Q(u) = L_G(v)$, v is denoted as a *candidate match* of u.

Strong simulation query [9]. We can then rewrite the semantics of strong simulation using matrices in Def. 1.

Definition 1. *A graph G is a strong simulation of a connected graph Q, denoted as $Q \prec_S G$, if G has a ball $B = G[v_s, d_Q]$, where $v_s \in V_G$, such that there exists a binary relation $S \subseteq V_Q \times V_B$, denoted by $\langle \cdot, \cdot \rangle$, satisfying the following conditions.*

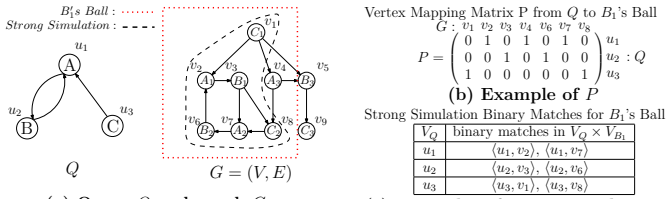

(a) Query Q and graph G

Vertex Mapping Matrix P from Q to B_1's Ball G : v_1 v_2 v_3 v_4 v_6 v_7 v_8

$$P = \begin{pmatrix} 0 & 1 & 0 & 1 & 0 & 1 & 0 \\ 0 & 0 & 1 & 0 & 1 & 0 & 0 \\ 1 & 0 & 0 & 0 & 0 & 0 & 1 \end{pmatrix} \begin{matrix} u_1 \\ u_2 : Q \\ u_3 \end{matrix}$$

(b) Example of P

Strong Simulation Binary Matches for B_1's Ball

V_Q	binary matches in $V_Q \times V_{B_1}$
u_1	$\langle u_1, v_2\rangle$, $\langle u_1, v_7\rangle$
u_2	$\langle u_2, v_3\rangle$, $\langle u_2, v_6\rangle$
u_3	$\langle u_3, v_1\rangle$, $\langle u_3, v_8\rangle$

(c) Examples of strong simulation

Fig. 2: A query, graph, and strong simulation

1) $\forall u \in V_Q$, $\exists v \in V_B$ *such that* $\langle u, v\rangle \in S$
2) $\exists u \in V_Q$ *such that* $\langle u, v_s\rangle \in S$
3) $\forall \langle u, v\rangle \in S$,
  (a) $L_Q(u) = L_B(v)$, *i.e.,* $P(u, v) = 1$.
  (b) for all $u' \in V_Q$ *where* $M_Q(u, u') = 1$, *there exists* v' *in* V_B *such that* $M_B(v, v') = 1$ *and* $\langle u', v'\rangle \in S$.
  (c) for all $u'' \in V_Q$ *where* $M_Q(u'', u) = 1$, *there exists* v'' *in* V_B *such that* $M_B(v'', v) = 1$ *and* $\langle u'', v''\rangle \in S$. □

A *strong simulation query* $Q = (V_Q, E_Q, \Sigma_Q, L_Q)$ on a graph $G = (V_G, E_G, \Sigma_G, L_G)$ computes whether there exists an S s.t. $Q \prec_S G$. Intuitively, S can be considered as a *match* from Q to B that preserves the topology of *both* children (3(b) of Def. 1) and parents (3(c) of Def. 1).

There have been related query semantics. Dual simulation [9] and graph simulation [7] do not restrict the matching in a ball. In addition, graph simulation only requires 3(b) of Def. 1. Matching queries of the *whole* graph in a ciphertext domain is computationally costly.

Example 2. *Fig. 2(a) are examples for query Q and graph G, whereas Fig. 2(b) is the vertex mapping matrix P from Q to ball $G[B_1, 2]$. Fig. 2(c) shows a binary match from Q to G such that $Q \prec_S G$.* □

B. Models and Problem Statement

System model. We follow the system model that is well-received in the database outsourcing literature shown in Fig. 3. We assume that the service provider (*SP*) is equipped with powerful computing utilities such as a cluster. The *SP* hosts a query service for publicly known graph data. The *SP* receives encrypted queries from a client, evaluates them in the encrypted domain, and returns the encrypted answers to the client. The *client* generates the encrypted queries, submits them to the *SP*, and decrypts the answers (the IDs of the balls that contain matchings). A storage server is specially introduced. If the client needs to determine the query matchings, the relevant encrypted balls are sent from the server. We assume that the *server* and the *SP* do not collude. Otherwise, the *SP* can infer the queries from the balls requested by the client.

The sequence of whole query processing is as follows: ⓘ→①→ⓘⓘ→②→③→④→ⓘⓘⓘ→ⓘⓥ. The key steps of privacy preserving query processing are ①, ②, ③, and ④, *i.e.*, the top half of Fig. 3. ① The *client* generates the encrypted messages of query graph and submits them to the *SP*. ② The *SP* evaluates a *client*'s encrypted query on the graph data and ③ returns the encrypted results to the *client*. ④ The *client* decrypts these results to obtain the final answer.

There are steps of ⓘ building and encrypting balls offline, storing them in a semi-honest storage server, and ⓘⓘ generating

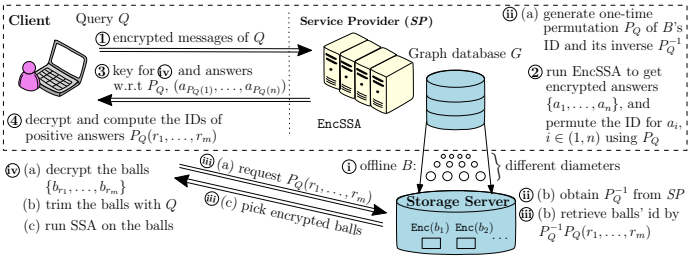

Fig. 3: The system model

the one-time permutation to be sent to the storage server for ⓘⓘⓘ the client to retrieve some encrypted balls from the storage server for ⓘⓥ verification of exact results. ⓘⓘ-ⓘⓘⓘ are introduced for a special case that the client could not know whether it has the whole graph. ⓘ-ⓘⓥ are standard techniques, and omitted.

Attack model. Assume the well known semi-honest adversary model [14], [17]–[19], where the attackers are honest but curious. For presentation simplicity, we consider the *SP* as the attackers. Also, we assume the attackers are the eavesdroppers and adopt the *chosen plaintext attack* (*CPA*) [14], *i.e.*, the adversaries can choose arbitrary plaintexts to obtain their ciphertexts to gain information to reduce the security.

Privacy target. To facilitate technical discussions, we assume that the privacy target is to protect the structures of the query graph Q from the *SP* under the attack model defined above. The structural information of Q is considered the *adjacency matrices* of Q. More specifically, the probability that the *SP* correctly determines the values of the adjacency matrix of the query graph Q is guaranteed to be lower than a threshold with reference to that of random guess.

Problem statement. *Given a strong simulation query Q and a large graph G, the system and attack model, we compute whether $Q \prec_S G$ by matching each ball of G to Q, while preserving the privacy target.*

III. Oblivious Strong Simulation Algorithm

In this section, we first present a transformed strong simulation algorithm *TSSA* based on the state-of-the-art and then propose an oblivious strong simulation algorithm *ObSSA* under the plaintext setting. We analyze the limitation of the encrypted version of *ObSSA*.

A. Transformed Strong Simulation Algorithm TSSA

The current state-of-the-art for determining strong simulation [9], *SSA*, starts with (candidate) matching query vertices to data vertices that have the same label and *iteratively prunes such matchings that have violations*.

Violation. Consider a binary match $\langle u, v\rangle \in V_Q \times V_G$ such that $L_Q(u) = L_G(v)$. There is a *violation* for $\langle u, v\rangle$ in a ball B if the topological constraints derived from 3(b) or 3(c) of Def. 1 (in Sec. II-A) *cannot* be satisfied.

1) For all $u' \in V_Q$ where $M_Q(u, u') = 1$, there exists v' in V_G such that $M_G(v, v') = 1$ and $\langle u', v'\rangle \in S$.
2) For all $u'' \in V_Q$ where $M_Q(u'', u) = 1$, there exists v'' in V_G such that $M_G(v'', v) = 1$ and $\langle u'', v''\rangle \in S$.

Algorithm 1: Transformed Strong Simulation Algorithm (*TSSA*)

Input : The adjacency matrix M_Q for the query Q, and the data graph G
Output: The strong simulation query result

```
1  result ← 0;                                          // 0: no valid matches
2  foreach vertex v in G with L_G(v) ∈ Σ_Q do
3      retrieve the ball B = G[v, d_Q] and represent it as an adjacency matrix
         M_B;
4      generate the vertex mapping matrix P from Q to B;
5      ViolationPruning (M_Q, M_B, P);
6      result ← result + CheckSS(P);
7  return result;
8  Procedure ViolationPruning(M_Q, M_B, P)
9  toDetect ← true;                          // more violations to detect
10 while toDetect do
11     toDetect ← false;
12     foreach (i, j) where P(i, j) = 1 do
13         foreach (i, k) where M_Q(i, k) = 1 do
14             if M_B(j) · P^T(k) = 0 then
15                 P(i, j) ← 0, toDetect ← true // Violation 1), SecIII-A
16         foreach (l, i) where M_Q(l, i) = 1 do
17             if P(l) · M_B^T(j) = 0 then
18                 P(i, j) ← 0, toDetect ← true // Violation 2), SecIII-A
19 Procedure CheckSS(P)
20 foreach row i in P do
21     if all the elements in P(i) equal to zero then
22         return 0;                                        // not a match
23     if all the elements in the column of the ball center v equal to zero then
24         return 0;                                        // not a match
25 return 1;                                               // a match
```

Algorithm 2: Oblivious Strong Simulation Algorithm (*ObSSA*)

Input : The data graph G, the adjacency matrix $\overline{M_Q}$ and the query Q
Output: The strong simulation query result

```
1  result ← 0;
2  foreach v in V_G, where L_G(v) ∈ Σ_Q do
3      retrieve the adjacency matrix M_B of the ball B = G[v, d_Q];
4      generate the vertex mapping matrix P from Q to B;
5      ObViolationPruning (M_Q-bar, M_B, P);
6      ObCheckSS(P);
7      result ← result + prod · sum_2;
8  return result;
9  Procedure ObViolationPruning(M_Q-bar, M_B, P):
10 generate R (of the same size as P) that contains 0s;
11 for n ← 0; n < |V_B| · |V_Q|; n++ do
12     //Violation detection
13     foreach P(i, j) do
14         R(i, j) ← Child (i,j);                          // Ref Eq. 1b
15         R(i, j) ← R(i, j)· Parent (i,j);                // Ref Eq. 1c
16     P ← R;
17 return P;
18 Procedure ObCheckSS(P):
19 prod ← 1, sum_2 ← 0;
20 foreach row i of P do
21     sum_1 ← 0;
22     foreach element P(i, j) in P(i) do
23         sum_1 ← sum_1 + P(i, j);
24     prod ← prod · sum_1;
25 foreach element P(i, j) in the column of the ball center do
26     sum_2 ← sum_2 + P(i, j);
27 return prod, sum_2;
```

The violation for $\langle u, v\rangle$ results in pruning of $\langle u, v\rangle$. When *no more* violations can be detected, *SSA* found a *valid* strong simulation *iff* (i) there is at least one match for each vertex in Q and (ii) B's center is matched to at least one vertex in Q.

Pseudo-code for *TSSA* (Alg. 1). The transformed strong simulation algorithm (*TSSA*) is presented in Alg. 1.[2] Alg. 1 returns a positive integer to show that $Q \prec_S G$, and it returns 0, otherwise. The details of Alg. 1 can be described as follows. For each vertex v in G with $L_G(v) \in \Sigma_Q$ required by Constraint 2 of Def. 1, Alg. 1 retrieves the adjacency matrix M_B that represents the ball[3] $B = G[v, d_Q]$ and constructs the vertex mapping matrix P from Q to B (Lines 3-4). For any vertex v_i in Q and any vertex v_j in B with the same label, $P(i, j) = 1$, *i.e.*, $\langle v_i, v_j\rangle$ is initially considered as a valid match. Fig. 2(b) shows an example for P. $P(3, 1) = 1$, since $L_Q(v_3) = L_G(v_1) = C$ as shown in Fig. 2(a).

In Line 5, `ViolationPruning` tests and prunes the invalid matches in P. In particular, for any element $P(i, j)$ in P (Line 12), if $P(i, j) = 1$ and there is a *violation* of the constraint 3(b) (resp. 3(c)) because of the children (resp. parents) as Line 14 (resp. Line 17), then Line 15 (Line 18) revises $P(i, j)$ to 0. Take Fig. 2(a) as an example. When matching u_1 in Q to v_4 in ball B_1, $P(1, 4)$ in Fig. 2(b) equals to 1 initially, and then, is revised to 0 since $P(2)\cdot M_B^{\mathrm{T}}(4) = 0$ for $M_Q(2, 1) = 1$ (Line 17), *i.e.*, no parents of v_4 in B_1 can satisfy Constraint 3(c), and thus, v_4 cannot be matched to u_1.

The algorithm repeats the above steps (Line 12) until no more violations can be detected and removed (Line 10). Then, `CheckSS` in Line 6 checks (i) whether the revised matrix P still satisfies Constraint 1 of Def. 1, *i.e.*, for the vertex v_i (the i^{th} vertex) in Q, there exists a vertex v_j (the j^{th} vertex) in B, such that $P(i, j)$ equals to 1. If there exists a row vector $P(i)$ equals to the zero vector (Line 21), there is no vertex in B that matches the i^{th} vertex in Q and Line 22 returns 0, *i.e.*, no match. `CheckSS` also checks (ii) whether the revised matrix P satisfies Constraint 2 of Def. 1, *i.e.*, for the ball center v, it can be matched to at least one vertex in Q. If all the elements in the column for the ball center equal to zero (Line 23), there is no vertex in Q that can be matched to the ball center and Line 24 returns 0, *i.e.*, no match. If Lines 21 and 23 do not hold, 1 is returned (Line 25). Following up with Example 2, (i) P shown in Fig. 2 does not have a row that contains all zeros and (ii) the column of the ball center (vertex 2) has a non-zero ($P(2, 3)$). Hence, G has a strong simulation in B (shown in the dotted box of Fig. 2(a)). Finally, Line 7 returns non-zero, *i.e.*, $Q \prec_S G$.

[2]To facilitate the discussion on obliviousness, Alg. 1 focuses on the core logic of *SSA*, *i.e.*, we omitted some optimizations that exploit query structures.

[3]The balls of some common radius values are built offline.

*B. Oblivious Strong Simulation Algorithm (*ObSSA*)*

In this subsection, we derive an oblivious algorithm called *ObSSA* from the transformed algorithm *TSSA*.

Violation detection. The core of *TSSA* is to remove the candidate matches that have the violations of Def. 1 Consider the vertex mapping matrix P from the query Q to the ball B. The value of $P(i, j)$ is modified using a series of addition and multiplication operations, called *violation detector*, as follows.

$$P(i,j)' = \mathsf{Child}(i,j)\cdot\mathsf{Parent}(i,j)\ , \quad \text{if} \quad P(i,j)\neq 0 \tag{1a}$$

$$\mathsf{Child}(i,j) = \prod_{k=1}^{|V_Q|}\Big[\overline{M_Q(i,k)} + \sum_{l=1}^{|V_B|}\big(M_B(j,l)P(k,l)\big)\Big] \tag{1b}$$

$$\mathsf{Parent}(i,j) = \prod_{k=1}^{|V_Q|}\Big[\overline{M_Q(k,i)} + \sum_{l=1}^{|V_B|}\big(M_B(l,j)P(k,l)\big)\Big], \tag{1c}$$

where $\overline{M_Q(i,k)} = 1 - M_Q(i,k)$ and $P(i,j)'$ denotes the modified value of $P(i,j)$ after running the violation detector.

Pseudo-code for ObSSA (Alg. 2). *ObSSA* is presented in Alg. 2. For each vertex v in G with $L_G(v) \in \Sigma_Q$, Line 3 retrieves the adjacency matrix M_B of the ball $B = G[v, d_Q]$ and Line 4 generates their vertex mapping matrix P from Q to B. Then, `ObViolationPruning()` (Lines 9-17) updates the matrix P iteratively for $|V_B| \cdot |V_Q|$ times using the violation detector (Eq. 1). Next, `ObCheckSS()` (Lines 18-27) computes the value prod and sum_2 indicating that whether $Q \prec_S B$. If prod or sum_2 equals to 0, then $B \subseteq G$ does not satisfy that $Q \prec_S G$. Otherwise, $Q \prec_S G$. Finally, Line 7 computes whether $Q \prec_S G$ or not.

Obliviousness of ObSSA. *Given queries of the same size and label set,* ObSSA *performs the same number and sequence of operations to evaluate each of them.* Firstly, *ObSSA* traverses the same balls. For each ball and each query, we can note that the sizes of the vertex mapping matrices Ps used in Line 4 are the same and independent to the query structure. In addition, regardless of the query structures, (i) the number of iterations in Line 11 of `ObViolationPruning()` are the same, and (ii) Eq. 1 (Lines 14-15), Lines 21-26 and Line 7 take the same number and sequence of additions and multiplications.

Correctness of ObSSA. We prove the correctness of *ObSSA* using two lemmas and a proposition.

Lemma 1. *Given a query Q to ball B,* `ObViolationPruning`$(\overline{M_Q}, M_B, P)$ *of* ObSSA *returns an P' such that $P'(i,j) = 0$ iff v_i in V_Q is not matched to v_j in V_B in a strong simulation relation.*

Proof. (Sketch). The lemma is established by a case analysis on Child w.r.t Tab. I. Case 4 is the only case that has a violation and Child yields 0. The analysis on Parent is similar. □

Proposition 1. ObSSA *returns non-zero iff there is a strong simulation between Q and B.*

Proof. (Sketch) By Lemma. 1, after `ObViolationPruning`, $P(i,j) = 0$ iff there is a violation for $\langle i,j \rangle$. In Line 24, the product of sum_1s can be non-zero only if for each $v_i \in Q$, there exists a match in B (*i.e.*, non-zero sum_1 in Line 24). In Line 26, the sum of all the elements in the column of the ball center can be non-zero only if there exists one vertex in Q that can be matched to the ball center (*i.e.*, non-zero $P(i,j)$ in Line 26). □

Example 3. *Following up with Example 2, Fig. 2(b) shows the initial P and Fig. 2(c) lists the non-zero entries in P' after the execution of* `ObViolationPruning()`. *A non-zero value of* prod *and* sum_2 *is returned by* `ObCheckSS()`. *Thus, ObSSA returns a non-zero* `result`*, which indicates $Q \prec_S G$.* □

Time complexity. Let N_{ball} denote the number of balls computed in Line 2. In `ObViolationPruning()`, Line 11 is repeated for $|V_B| \cdot |V_Q|$ times. Assume that both the addition and multiplication operations take $O(1)$ time. Then, Eq. 1 takes $O(|V_Q| \cdot |V_B|)$ time. Since there are $|V_Q| \cdot |V_B|$ elements in matrix P to be computed using Eq. 1, `ObViolationPruning()` needs $O(|V_Q|^3 \cdot |V_B|^3)$ time. For `ObCheckSS()`, computing prod and sum_2 needs $O(|V_Q| \cdot |V_B|)$ time. Hence, the total time complexity is $O(N_{ball} \cdot (|V_Q|^3 \cdot |V_B|^3))$.

C. Encoding and Encryption

To make *ObSSA* secure, we present the encoding for the matrices and adopt a partial homomorphic encryption scheme (*PHE*) to facilitate secure matrix computations.

Encoding for $\overline{\mathbf{M_Q}}$. $\forall i,j \in [1, |V_Q|]$, $\overline{M_Q(i,j)}$ is encoded as follows.

$$\overline{M_{Q_E}(i,j)} = \begin{cases} q, & \text{if } \overline{M_Q(i,j)} = 0; \text{ and} \\ 1, & \text{otherwise,} \end{cases}$$

where q is a large prime number. Based on this encoding, we use a symmetric encryption scheme called *cyclic group based encryption* (*CGBE*) [20] to encrypted the encoding for $\overline{M_Q}$. Fully homomorphic encryption scheme (*FHE*) [13] is not adopted because of their efficiency problem. *CGBE* is a *partially homomorphic encryption* scheme supporting both additions and multiplications but the scheme is correct only when the computed ciphertext corresponds to a plaintext that does not exceed a predefined limit.

Encryption. We now recall the definition of *CGBE*, namely the key generation `Gen`, encryption `Enc`, decryption `Dec` functions as follows.

- `Gen`. `Gen` generates a cyclic group $\langle g \rangle = \{g^i | i \in \mathbb{Z}_p, g^i \in \mathbb{Z}_n\}$ with the generator g and order p ($p \gg q$). Note that p should be a large prime number. Moreover, `Gen` generates a uniformly random secret key $x \in [1,p]$. It outputs p as the public value for the computation on *SP* and (x,g) as the private keys.
- `Enc`. `Enc` takes a message m and the secret key (x,g) as input, chooses a random value r and produces the ciphertext c as output, as follows,

$$c = mrg^x \pmod p.$$

- `Dec`. `Dec` takes a ciphertext c and the secret key (x,g) as input and computes the decrypted message as output, as follows,

$$mr = cg^{-x} \pmod p.$$

Note that `Dec` only decrypts the ciphertext c as a product of message m and a random value r, where r is different for each ciphertext. We use the following to encrypt the encoding of $\overline{M_Q}$.

$$mr = \begin{cases} 0 \pmod q, & \text{which encrypts the plaintext 0;} \\ \mathbb{Z}^+ \pmod q, & \text{which encrypts the plaintext 1.} \end{cases}$$

As discussed in [20], there is a negligible chance of false positives that $\mathbb{Z}^+ = 0 \pmod q$, since q is a large prime number. Moreover, *CGBE* is correct only if the computed ciphertext corresponds to a plaintext not larger than the order p. Otherwise, there is an overflow.

D. Encrypted ObSSA and its Limitations

Using the encoding and encryption schemes, we describe an encrypted *ObSSA* algorithm, and analyze its limitations.

TABLE I: The truth table for matching a vertex v_i of the query to a vertex v_j of the ball via a case analysis on v_i's child v_k

	$\overline{M_Q(i,k)}$	$\sum_{l=1}^{\lvert V_B\rvert}\big(M_B(j,l)\cdot P(k,l)\big)$	$P(i,j)'$
Meaning of values	0:$(i,k)\in E_Q$ 1:$(i,k)\notin E_Q$	0:v_k is not matched $\mathbb{Z}^+$:v_k is matched	0:violation $\mathbb{Z}^+$: valid
Case 1. (i, k) missing; and v_k matched	1	$\mathbb{Z}^+$	$\mathbb{Z}^+$
Case 2. (i, k) missing; and v_k not matched	1	0	$\mathbb{Z}^+$
Case 3. (i, k) present & matched	0	$\mathbb{Z}^+$	$\mathbb{Z}^+$
Case 4. (i, k) present but v_k not matched	**0**	**0**	**0**

Encrypted ObSSA. In encrypted *ObSSA*, the adjacency matrix of Q is encrypted by the client. G is encoded for correct computation. The encrypted *ObSSA*, the ball and the vertex mapping matrix are generated by the *SP* as in *ObSSA*. In Line 5 (Lines 9-17), each element $P(i,j)\in P$ is computed iteratively $|V_B|\cdot|V_Q|$ times. If the size $|V_B|$ of ball B is large, it not only takes a long runtime but also makes the value of the plaintext for the encoding $P(i,j)$ large. The following steps illustrate the first two iterations of `ObViolationPruning`. Denote P_i to be the computed vertex mapping matrix P after the i-th iteration, and P_0 is P.

1) The encrypted query $\overline{M_{Q_E}}$, denoted as $\overline{M_{Q_{Enc}}}$, contains g^x. To achieve homomorphic computation on Eq. 1 in each iteration (Lines 11-16) for correct decryption in the end (Line 17), each polynome of $\sum_{l=1}^{|V_B|}\big(M_B(j,l)\cdot P_0(k,l)\big)$ must contain the same power of $g^{x\propto}$ with $\overline{M_{Q_{Enc}}}$, where $\propto$ is a value derived from the iteration number.

2) The first iteration of `ObViolationPruning` is different from the others. Note that the initial matrix P_0 contains plaintext. *SP* can replace the possibly large *plaintext* value of $\sum_{l=1}^{|V_B|}\big(M_B(j,l)\cdot P_0(k,l)\big)$ with the chosen ciphertexts of 0 and 1, denoted by c_0 and c_1, respectively, provided by the client. If $\sum_{l=1}^{|V_B|}\big(M_B(j,l)\cdot P_0(k,l)\big)$ is a non-zero, *SP* replaces it with c_1, and otherwise, c_0.

3) The remaining iterations are done in the ciphertext domain.

Overflow in ciphertext for its plaintext value.

1) The largest possible value of P_1 can be analyzed as follows. Recall `Enc` of *CGBE*. The ciphertext is either g^xr or g^xrq, which corresponds to 1 or 0, and each ciphertext contains the secret key g^x. W.l.o.g, we analyze the computation for Child in Eq. 1. Consider the largest possible value of Child in the first iteration, *i.e.*, each ciphertext has the largest value g^xrq. Then, the value of Child is as follows.

$$\prod_{k=1}^{|V_Q|}(g^xrq+g^xrq)=\big[(g^x)^{|V_Q|}\big]\cdot(2rq)^{|V_Q|}$$

2) In the second iteration, we ensure the two components of Child (Eq. 1b) have the same order of g^x, so that they can be correctly added. First, $\sum_{l=1}^{|V_B|}\big(M_B(j,l)\cdot P_1(k,l)\big)$ contains the power of the private key $(g^x)^{2|V_Q|}$. Second, we replace $\overline{M_{Q_{Enc}}(i,j)}$ with $\overline{M_{Q_{Enc}}(i,j)}^{|V_Q|}$. As a consequence, after the second iteration, the largest possible value of $P_2(i,j)$ is the following.

$$P_2(i,j)=\big[(g^x)^{4|V_Q|^2}\big]\cdot\big[(rq)^{2|V_Q|}+|V_B|\cdot(2rq)^{2|V_Q|}\big]^{2|V_Q|},$$

where $\big[(rq)^{2|V_Q|}+|V_B|\cdot(2rq)^{2|V_Q|}\big]^{2|V_Q|}$ corresponds to the plaintext of the largest possible value for $P_2(i,j)$, which is larger than $(2rq)^{4|V_Q|^2}$.

For example, consider the experimental settings of [20] and [16]. We assume that both q and r are of 32 bits. If the public value p is of 4096 bits and the size $|V_Q|$ of the query is 5, $(2rq)^{4|V_Q|^2}$ needs 6500 bits.

3) Similar to the second iteration, we can analyze that Child of the nth iteration contains a factor $(g^x)^{(2|V_Q|)^n}$.

From the above analysis, we can observe that in practice, the value of the plaintext can be larger than the order p of *CGBE* and there can be an overflow.

IV. A Practical Inexact Solution *EncSSA*

Due to the limitation discussed in Sec. III-D, we propose a practical, inexact algorithm, called *EncSSA*, which comprises three pruning ideas, namely, localized pruning, neighbor-label pruning, and path pruning.

A. Localized Violation Pruning

Localized violation pruning (presented in Alg. 3 `TwoIterPruning`) contains two main techniques. Firstly, we conduct *violation detection* for a bounded number of times. Secondly, we replace large ciphertext with small ciphertext to allow more violation detections before overflow happens.

We illustrate the techniques with an example of Child, shown in Fig. 4(a). (The case of Parent is similar.) We also denote $G[v_2,2]$ as B. Alg. 3 checks whether a match from $u_1\in V_Q$ to $v_2\in V_B$ violates Def. 1, *i.e.*, conducting the *violation detector* on $P_0(1,2)$.

In the first iteration (Lines 3-8) of Alg. 3, Line 5 computes the value of $\mathsf{Child}(1,2)$ in Eq. 1(b). Then, Line 6 searches for the value of $\mathsf{Child}(1,2)$ in the column of the original ciphertext in the replacement table shown in Fig. 4(b) and updates $\mathsf{Child}(1,2)$ with the corresponding ciphertext for replacement. The rows of the replacement table in Fig. 4(b) list all the possible cases of Child. (The replacement table has $2^{|V_Q|-1}$ rows.) As the term $\overline{M_{Q_{Enc}}(i,j)}$ of Eq. 1(b) is computed and provided by the client to *SP*, the client can also precompute a ciphertext that corresponds to a small plaintext for replacement.

The second iteration (Lines 9-12) conducts violation detection for the second time. It takes the encrypted vertex mapping matrix P_1 as input. Hence, Alg. 3 performs violation pruning in the encrypted domain to yield P_2.

Analysis of query size and overflow. In Fig. 4(b), the value of Child is at most g^xrq. Therefore, the value of each element in P_1 is at most $g^{2x}(rq)^2$ (Lines 7-8). With Eq. 1, we know that the value of each element in P_2 is:

$$P_2(i,j)\le\big[(g^x)^{4|V_Q|}\big]\cdot\big[(rq)^2+|V_B|\cdot(2rq)^2\big]^{2|V_Q|}$$

Assume that both q and r are of 32 bits and the public order p of *CGBE* is of 4096 bits. If $|V_B|$ needs 20 bits, then,

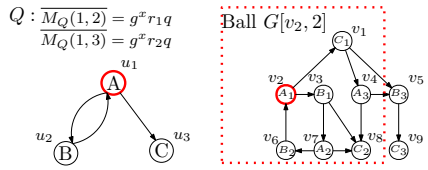

(a) Q, the ball, and checking matching from u_1 to v_2

Cases of possible values of Child for u_1	Original ciphertext	Replacement	Violation
1. $(\overline{M_Q(1,2)} + c_0) \cdot (\overline{M_Q(1,3)} + c_0)$	$(g^x r_1 q + c_0) \cdot (g^x r_2 q + c_0)$	$g^x rq$	Yes
2. $(\overline{M_Q(1,2)} + c_0) \cdot (\overline{M_Q(1,3)} + c_1)$	$(g^x r_1 q + c_0) \cdot (g^x r_2 q + c_1)$	$g^x rq$	Yes
3. $(\overline{M_Q(1,2)} + c_1) \cdot (\overline{M_Q(1,3)} + c_0)$	$(g^x r_1 q + c_1) \cdot (g^x r_2 q + c_0)$	$g^x rq$	Yes
...	...	...	...
$2^{\lvert V_Q\ 1\rvert}$. $(\overline{M_Q(1,2)} + c_1) \cdot (\overline{M_Q(1,3)} + c_1)$	$(g^x r_1 q + c_1) \cdot (g^x r_2 q + c_1)$	$g^x r$	No

(b) Replacement table for u_1's children

Fig. 4: (a) The example query, ball and matching; and (b) the replacement table $\mathcal{T}_R$ of large ciphertext with small ciphertext

Algorithm 3: Localized violation pruning `TwoIterPruning`

Input : The replacement tables $\mathcal{T}_R$ of Q, the initial vertex mapping matrix P_0 and the adjacency matrix M_B
Output: The vertex mapping matrix R_1 after two iterations of violation detections (cf. `ObViolationPruning` of Alg. 2)

```
1  Procedure TwoIterPruing(T_R, P_0, M_B):
2  generate two null matrices P_1 and R_1 of the same size as P_0;
3  foreach element P_0(i, j) do                          // 1st iteration
4      if P_0(i, j) ≠ 0 then
5          compute the values of Child and Parent;       // Eq.1b and 1c
6          Search the replacement tables T_R for both v_i's children and
             parents, then replace Child and Parent with small ciphertext;
7          P_1(i, j) ← Child;
8          P_1(i, j) ← P_1(i, j)· Parent;
9  foreach element P_1(i, j) do                          // 2nd iteration
10     if P_1(i, j) ≠ 0 then
11         R_1(i, j) ← Child;
12         R_1(i, j) ← R_1(i, j)· Parent;
13 return R_1;
```

TABLE II: The encrypted 3-path table $\mathcal{T}_P$ (partial)

3-path p_i starting from u_1	ciphertext c_{p_i}	plaintext	meaning
p_1. (A, B, C)	$g^x r$	$\mathbb{Z}^+$	not exists
p_2. (A, C, B)	$g^x r$	$\mathbb{Z}^+$	not exists
3-path p_i starting from u_2	ciphertext c_{p_i}	plaintext	meaning
p_1. (B, A, C)	$g^x rq$	0	exists
p_2. (B, C, A)	$g^x r$	$\mathbb{Z}^+$	not exists

by substituting these number into the above formula and some arithmetics, we have `TwoIterPruning` can support the query size up to 13 (detailed derivations in [21]).

$$|V_B| \cdot 2^{302|V_Q|} < 2^{4096} \quad \Rightarrow \quad |V_Q| \leq \lfloor \frac{4076}{302} \rfloor = 13.$$

Time complexity and correctness. Alg. 3 conducts two iterations of violation detection instead of $|V_Q| \cdot |V_B|$ iterations in Alg. 2. Therefore, the time complexity of Alg. 3 is $O(|V_Q|^2 \cdot |V_B|^2)$. Regarding the correctness, since Alg. 3 conducts two iterations of violation detection, Alg. 3 indicates no violations for the balls having matches as well as some balls that do not have matches (false positives).

B. Path-based Pruning

In the Sec. IV-A, we present localized pruning that makes use of the information of 2-hop neighbors. In this subsection, we propose a path-based pruning method making use of neighbors reachable from larger hops.

We call k-path a directed path of $k-1$ edges of distinct vertex labels. An example of 3-path in Fig 2(a) is $u_2 \rightarrow u_1 \rightarrow u_3$ and its label sequence is (B, A, C). The following proposition can be established from Def. 1.

Proposition 2. *Given a query Q and a ball B in a graph G with the center v, and any vertex u in Q, where $L_Q(u) = L_G(v)$, if there exists at least one k-path p starting from u in Q but not from v in B, then u cannot be matched to v.*

Prop. 2 is then used to prune balls that must contain violations due to the balls' centers. We illustrate the steps of pruning with 3-path as follows.

- *Client*: For each vertex u of Q, the client enumerates all possible k-paths starting from u using $|\Sigma_Q|$ labels. For example, given Q as shown in Fig. 2(a), the client computes an encrypted 3-path table $\mathcal{T}_P$ of all the $|V_Q| \cdot A_2^2 = 6$ possible 3-paths, where A is the permutation symbol, as Tab. II shows some of them. For each 3-path p in $\mathcal{T}_P$, there is a ciphertext corresponding to a plaintext indicating that whether p exists in Q. Then, the client sends $\mathcal{T}_P$ to the *SP*.
- *SP*: After receiving table $\mathcal{T}_P$, for each ball B, the *SP* runs `PathPruning` (Alg. 4). Line 3 first uses *DFS* to traverse ball B and find all the 3-paths starting from the center v_j of B. For each vertex u_i in Q that potentially matches v_j, Lines 5-11 aggregate the ciphertexts in C_i for pruning B.

Specifically, for each k-path p starting from u_i (Line 6), if there exists k-path p starting at v_j (Line 7), too, then, Line 8 multiplies C_i with the ciphertext of 1, which is used to ensure the power of the private key $g^{x \cdot A^{k-1}_{|\Sigma_Q|-1}}$ for the correctness of decryption. Otherwise, in Line 10, by Prop. 2, p leads to violation if u_i has p. Hence, C_i is multiplied by the ciphertext c_p of p in $\mathcal{T}_P$ (Line 10). Line 11 aggregates the ciphertexts C_is of all possible matching vertices into R_2. If $\texttt{Dec}(R_2) = 0$, *i.e.*, B's center v_j cannot be matched to any vertices in Q, then B is pruned. The generalization of path-based pruning including k-paths ending at each vertex is immediate.

Analysis. Given queries with the same $|V_Q|$, Σ_Q and L_Q, Alg. 4 conducts the same operations without exploiting the query structure. Thus, Alg. 4 is oblivious. Regarding the value of k, the pruning of `PathPruning` when $k = 2$ is covered by `TwoIterPruning`. Hence, we assume $k > 2$, but $k \leq |V_Q|$.

Regarding the overflow problem due to *CGBE*, we remark that Lines 8 and 10 in Alg. 4 use multiplications for $A^{k-1}_{|\Sigma_Q|-1}$ times in total. In the experimental settings in Sec. VI, both q and r are of 32 bits while the public value p is of 4096 bits. Hence, $\lfloor 4096/64 \rfloor = 64$ times of multiplication are supported. If $A^{k-1}_{|\Sigma_Q|-1} > 64$, we can do the multiplications in batches.

Alg. 4 uses $O(|V_B|+|E_B|)$ time for *DFS* and $O(|V_Q| \cdot A^{k-1}_{|\Sigma_Q|-1} \cdot k \cdot D_B)$ time for ciphertext aggregation in the worst case, where D_B is the maximum degree of B.

C. Neighbor-Label Pruning

In previous subsections, we use Child and Parent to check two-hop neighbors and k-path to check neighbors that are further away. Here, we propose to use simpler information (just labels) to detect violations due to the neighbors even further away, and yet we do not run into the overflow problem.

Algorithm 4: Path-based pruning `PathPruning`

Input : The length k, the encrypted k-path table $\mathcal{T}_P$, the adjacency matrix M_B and the vertex mapping matrix P
Output: The encrypted messages R_2 for pruning ball B

1 **Procedure** `PathPruning(` $\mathcal{T}_P$, M_B`)`:
2 $R_2 \leftarrow 0$;
3 start a *DFS* from B's center v_j to compute all k-paths;
4 **foreach** u_i in Q where $P(i,j) = 1$ **do**
5 $C_i \leftarrow 1$;
6 **foreach** *k-path* p in $\mathcal{T}_P$ starting at u_i **do**
7 **if** p is found that starts at v_j **then**
8 $C_i \leftarrow C_i \cdot c_1$; `// aggregate ciphertext of 1`
9 **else**
10 $C_i \leftarrow C_i \cdot c_p$; `// violation if` u_i `has` p
11 $R_2 \leftarrow R_2 + C_i$;
12 **return** R_2;

Algorithm 5: Neighbor-label pruning `NLPruning`

Input : The hop h, the *NL-index* NL^h, the center v of ball B and the encrypted *NL-matrix* $\overline{EM_Q^h}$
Output: The encrypted messages R_3 for pruning ball B

1 **Procedure** `NLPruning(`$\overline{EM_Q^h}$, NL^h`)`:
2 **foreach** u_i in Q with $L_Q(u_i) = L_G(v)$ **do**
`// detect violation using Prop.3`
3 $C_i \leftarrow 1$;
4 **for** the $j^{\text{th}}(1 \le j \le |\Sigma_Q|)$ label l in Σ_Q **do**
5 **if** $l \in NL^h(v)\}$ **then**
6 $C_i \leftarrow C_i \cdot c_1$; `// aggregate ciphertext of 1`
7 **else**
8 $C_i \leftarrow C_i \cdot \overline{EM_Q^h(i,j)}$; `// violation if` $l \notin NL^h(v)$
9 $R_3 \leftarrow R_3 + C_i$;
10 **return** R_3;

NL-index. Given a vertex u in G and a hop number h, we precompute the h-hop neighbors $N = \{v | \mathsf{dis}(u,v) = h\}$. Then, the h-hop *NL-index* of u, denoted by $NL^h(u)$, is the labels of the h-hop neighbors, *i.e.*, $NL^h(u) = \{L_G(v) | v \in N\}$.

Example 4. *Consider the graph G in Fig. 2(a). $NL^6(v_2) = \{L_G(v_3), L_G(v_8), L_G(v_7)\} = \{A, B, C\}$.*

NL-matrix. Given a query Q and a hop number h, the *NL-matrix* of Q for h-hop neighbors (exclude cycles), denoted as $\overline{M_Q^h}$, is a $|V_Q| \times |\Sigma_Q|$ matrix defined as follows: $\overline{M_Q^h(i,j)}$ = 0 if the vertex v_i has an h-hop neighbor; and 1 otherwise.

Based on *NL-index* and *NL-matrix*, we propose the following proposition to detect violations.

Proposition 3. *Consider a query Q and a ball B with the center v and any vertex u in Q, where $L_Q(u) = L_G(v)$. If u has an h-hop neighbor that has a label l, but $l \notin NL^h(v)$, then u cannot be matched to v.*

Since the hop in *NL-matrix* excludes cycles whereas the h-hops in *NL-index* includes cycles, Prop. 3 holds and it can be easily proved by following Def. 1. We propose the `NLPruning` procedure (Alg. 5). `NLPruning` takes the hop number h, the *NL-index* and the encrypted *NL-matrix* as inputs, and outputs encrypted messages R_3 as the violation detection result.

For each vertex u_i in Q having the same label as the ball center v (Line 2), Lines 4-8 aggregate the ciphertexts in C_i for pruning B. Specifically, for each label l in Σ_Q (Line 4), if v can reach an h-hop neighbor that has label l (Line 5), then Line 6 multiplies C_i by the ciphertext of 1, to ensure correctness of decryption. Otherwise, in Line 8, there may be a violation for the unreachable h-hop label l by Prop. 3. Assumed that l is the j^{th} label in Σ_Q, Line 8 multiplies C_i by $\overline{EM_Q^h(i,j)}$. If u_i has an h-hop neighbor with label l, then $\mathtt{Dec}(\overline{EM_Q^h(i,j)}) = 0$ and hence, $\mathtt{Dec}(C_i) = 0$. Otherwise, $\mathtt{Dec}(C_i) = \mathbb{Z}^+$. Line 9 aggregates the ciphertexts C_is into R_3. If $\mathtt{Dec}(R_3) = 0$, *i.e.*, B's center v cannot be matched to any vertices in Q, then B can be pruned.

Algorithm 6: *EncSSA* Algorithm

Input : The data graph G, the encrypted adjacency matrix $\overline{EM_Q}$, the diameter d_Q, portion p, the replacement tables $\mathcal{T}_R$, length k with the encrypted k-path tables $\mathcal{T}_P$, hop h with the encrypted *NL-matrices* $\overline{EM_Q^h}$ and the *NL-indexes* NL^h
Output: A superset R_S of balls containing the strong simulation results

At the *SP* side:
1 **foreach** v in V_G, where $L_G(v) \in \Sigma_Q$ **do**
2 retrieve the adjacency matrix M_B of the ball $B = G[v, d_Q]$;
3 generate the vertex mapping matrix P_0 from Q to B;
4 initialize R_0, R_1, R_2 and R_3;
5 `BallPruning(`$M_B, P_0, p, \mathcal{T}_R, k, \mathcal{T}_P, h, \overline{EM_Q^h}, NL^h$`)`;
6 `ResultAggregation()`;
7 send to the client the ciphertexts R_0^is, R_1^is, R_2s and R_3s, $i \in [1, |V_Q|]$ for all balls;

Procedure `BallPruning(`$M_B, P_0, p, \mathcal{T}_R, k, \mathcal{T}_P, h, \overline{EM_Q^h}, NL^h$`)`:
8 $R_0 =$ `OneIterPruning(`M_B, P_0`)`; `// 1-hop pruning`
9 $R_1 =$ `TwoIterPruning(`$\{T_R\}$, M_B, P_0, p`)`; `// 2-hop`
10 $R_2 =$ `PathPruning(`$\{\mathcal{T}_P\}$, M_B, k`)`; `// 3∼`k`-hops`
11 $R_3 =$ `NLPruning(`$\overline{EM_Q^h}$, NL^h, h`)`; `// `k`∼`h`-hops`

Procedure `ResultAggregation()`:
12 **foreach** *row* $i \in [1, |V_Q|]$ **do**
13 $R_0^i = \sum_{\text{column}=1}^{|V_B|} R_0(i, \text{column})$;
14 $R_1^i = \sum_{\text{column}=1}^{|V_B|} R_1(i, \text{column})$;
15 $R_0^{'} = \sum_{\text{row}=1}^{|V_Q|} R_0(\text{row, column for ball center})$;
16 $R_1^{'} = \sum_{\text{row}=1}^{|V_Q|} R_1(\text{row, column for ball center})$;

At the *Client* side when $R_0^{'}$, $R_1^{'}$, R_0^i, R_1^i, R_2 and R_3 are received from the *SP*:
Procedure `Decryption(`$R_0^{'}$, $R_1^{'}$, R_0^i, R_1^i, R_2, R_3`)`:
17 **foreach** $R_0^{'}$, $R_1^{'}$, R_0^i, R_1^i, R_2, R_3 belonging to the same ball B **do**
18 **if** `Dec(`R_2`)` $= 0$ **then** `// Alg. 4 in Sec. IV-B`
19 **continue**;
20 **if** `Dec(`R_3`)` $= 0$ **then** `// Alg. 5 in Sec. IV-C`
21 **continue**;
22 **if** $\prod_{i=1}^{|V_Q|}$ `Dec(`R_0^i`)` $= 0$ || $\prod_{i=1}^{|V_Q|}$ `Dec(`R_1^i`)` $= 0$ **then**
`// similar to Line 24 in ObCheckSS() in Alg. 2`
23 **continue**;
24 **if** `Dec(`$R_0^{'}$`)` $= 0$ || `Dec(`$R_1^{'}$`)` $= 0$ **then**
`// similar to Line 26 in ObCheckSS() in Alg. 2`
25 **continue**;
26 ball B is added into R_S;

Analysis. The value of h for Alg. 5 should be larger than k for k-path in Sec. IV-B to further prune the balls that cannot be pruned by Alg. 4. The analysis of the obliviousness of Alg. 5 and the overflow in Alg. 5 are similar to the one of Alg. 4. Regarding the worst-case time complexity, Alg. 5 takes $O(|V_Q| \cdot |\Sigma_Q| \cdot \max\{|NL^h(v)|\})$.

D. EncSSA Algorithm

In this subsection, to answer the strong simulation query, we propose an encrypted inexact algorithm, called *EncSSA*, using the pruning techniques of Sec. IV-A, IV-B and IV-C.

Pseudo-code for EncSSA (Alg. 6). Taking the data graph G, the encrypted adjacency matrix $\overline{EM_Q}$, the diameter d_Q, portion p and the inputs of Alg. 3, 4, 5 as inputs, the *EncSSA*

algorithm outputs a superset R_S of balls that contains the strong simulation results for Q. At the *SP* side, for each vertex v in G, Line 2 retrieves the adjacency matrix M_B for the ball $B = G[v, d_Q]$ and Line 3 generates the corresponding vertex mapping matrix P_0 from Q to B. Then, the `BallPruning()` procedure (Line 5) computes the ciphertexts for pruning B. Specifically, Line 8 conducts the violation detection on all vertices in B for only one iteration (*i.e.*, Lines 3-8 in Alg. 3), which is denoted as `OneIterPruning()`. Then, Line 9 randomly chooses a portion p ($0 < p \leq 1$) of vertices among $|V_B|$ and conducts Alg. 3 on these vertices. Line 10 conducts Alg. 4 and Line 11 conducts Alg. 5. Since R_0 and R_1 obtained by Lines 8-9 are matrices, the `ResultAggregation()` procedure (i) combines the ciphertexts in each row of both matrices by addition (Lines 12-14), and (ii) combines the ciphertexts in the column for the ball center by addition (Lines 15-16). Finally, the *SP* sends the combined ciphertexts together with R_2 and R_3 to the client (Line 7).

At the client side, after receiving the ciphertexts, `Decryption()` first decrypts the ciphertext R_2 (R_3) and prunes B based on Alg. 4 (Alg. 5) in Line 18 (Line 20). Then, similar to `ObCheckSS()` in Alg. 2, (i) Line 22 checks whether there exists at least one valid match in B for each vertex in Q and (ii) Line 24 checks whether there exists at least one vertex in Q that can be matched to the ball center. If B cannot be pruned, Line 26 adds B into R_S.

Analysis. As introduced in Sec. IV-A, IV-B and IV-C, *EncSSA* can handle the situation of overflow. Moreover, the computations at the *SP* side consist of Alg. 3-5, which are oblivious. Then, we analyze the scale of ciphertexts need in *EncSSA*. Let N_{ball} denote the number of balls computed in Line 1. For each ball, Lines 10-11 (Lines 15-16) both generate $O(1)$ ciphertexts while Lines 13-14 both generate $|V_Q|$ ciphertexts. Therefore, *EncSSA* needs to transmit in total $N_{ball} \cdot (a \cdot |V_Q| + b)$ ciphertexts, where $1 \leq a, b \leq 2$, in practice. Regarding time complexities, *EncSSA* needs $O\big(N_{ball} \cdot (|V_Q|^2 \cdot |V_B|^2 + |E_B| + |V_Q| \cdot A_{|\Sigma_Q|-1}^{k-1} \cdot k \cdot D_B + |V_Q| \cdot |\Sigma_Q| \cdot \max\{|NL^h(v)|\})\big)$ time at the *SP* side, and $O(N_{ball} \cdot |V_Q| \cdot Dec_t)$ at the *client* side, where Dec_t is the time for decrypting a ciphertext.

V. PRIVACY ANALYSIS

Due to space restrictions, we present the main ideas of the privacy analysis, but present the detailed derivations in [21].

Lemma 2. *CGBE [20] is secure against CPA. $\overline{EM_Q}$ and $\overline{EM_Q^h}$ is preserved from SP against the attack model.*

Proposition 4. *The structure of query encrypted by CGBE is preserved from SP against the attack model.*

With Lemma 2 and Prop. 4, *SP* cannot attack the query's ciphertext directly. Then, we analyze Alg. 3-Alg. 5.

For Alg. 3, assume that the vertex mapping matrix has n elements with value 1. Let $\mathcal{A}(Q)$ be a function that returns 1 if *SP* can determine the existence of an edge of Q, and 0 otherwise. Then, since Alg. 3 conducts oblivious computation on ciphertexts encrypted by *CGBE*, we can yield Prop. 5.

TABLE III: Statistics of the real-world datasets

Graph G	$\lvert V_G\rvert$	$\lvert E_G\rvert$	Σ_G
Slashdot	82,168	948,464	32, 64, 128
DBLP	317,080	1,049,866	32, 64, 128
Twitter	81,306	1,768,149	32, 64, 128

Proposition 5. *After running* `TwoIterPruning`, $Pr[\mathcal{A}(Q) = 1] \leq 2^{-n}$.

Prop. 5 states that there is a negligible probability that *SP* can attack the vertex mapping matrix after conducting the localized violation pruning.

For Alg. 4 (resp. Alg. 5), let $\mathcal{G}(R_2)$ (resp. $\mathcal{K}(R_3)$) returns 1 if *SP* can compute the plaintext of the output ciphertext R_2 (resp. R_3), and 0, otherwise. We analyze the possibilities of $\mathcal{G}(R_2)$=1 (resp. $\mathcal{K}(R_3)$=1) and yield Prop. 6 (resp. Prop. 7).

Proposition 6. *After running* `PathPruning`, $Pr[\mathcal{G}(R_2) = 1] \leq 1/2 + \epsilon$, *where ϵ is negligible.*

Proposition 7. *After running* `NLPruning`, $Pr[\mathcal{K}(R_3) = 1] \leq 1/2 + \epsilon$, *where ϵ is negligible.*

Prop. 6 (resp. Prop. 7) states that there is a negligible probability *SP* can do so after conducting the path-based pruning (resp. neighbor-label pruning). In addition, we yield Prop. 8 to show that *SP* cannot infer the plaintext of the structural information of the query from the relations between the encrypted messages of different hops (*e.g.*, the 1-hop adjacency matrix can yield the 2-hop adjacency matrix) needed for neighbor-label pruning. Note that no relations exist in the case for localized violation pruning (path-based pruning).

Proposition 8. *Given the encrypted matrices $\overline{EM_Q}$ and $\overline{EM_Q^h}$, the neighbor information of the query is preserved from SP against the attack model under CGBE.*

Putting Props. 5, 6, 7 and 8 together, we have Thm. 1 since the three pruning techniques used independently in *EncSSA*.

Theorem 1. EncSSA *(Alg. 6) preserves the privacy of the query structure against* CPA.

VI. EXPERIMENTAL RESULTS

We conducted detailed experiments to investigate the efficiency and effectiveness of our proposed algorithms.

Platform. The prototype[4] used in the experiment is implemented in C++. We used a machine with an Intel Xeon E5-2630 2.2GHz CPU and 256GB RAM running CentOS 7.7 for both the *SP* and *client*. We used the GMP libraries to implement *CGBE* encryption scheme.

Datasets. We used three real-world datasets, namely *Slashdot*, *DBLP* and *Twitter* [22]. Some characteristics of the datasets can be found in Tab. III. Since the vertices in these datasets do not have labels, similar to [9], we generated random labels for them. We use the subscript $|\Sigma_G|$ to denote the generated datasets, *i.e.*, *Slashdot*$_{|\Sigma_G|}$, *DBLP*$_{|\Sigma_G|}$ and *Twitter*$_{|\Sigma_G|}$.

Query sets. Given a query size $|V_Q|$ and a diameter d_Q, the

[4] https://github.com/PP-StrongSimulation?tab=repositories

TABLE IV: Statistics of the balls of random queries ($\Sigma = 64$)

Dataset	# of balls (Bs)	average $\|V_B\|$	stddev $\|V_B\|$
Slashdot	4489	481	498
DBLP	4761	77	55
Twitter	5964	931	848

query generator *QGen*[4] derived a radius γ. *QGen* randomly chose a vertex v in the data graph and obtained the induced graph of v's 1 to γ-hop neighbors. After random edge deletions, *QGen* output the maximum connected component if it had a size $|V_Q|$ and diameter d_Q.

Default parameters. The parameters are described as follows:

- *CGBE*. The encoding q and random number r for CGBE were both of 32 bits. The public value was of 4096 bits.
- *Query and graph*. The query sizes $|V_Q|$ varied from 6 to 10. The default value of $|V_Q|$ was 8. According to the analysis in Sec. IV-A, the parameters for CGBE can support $|V_Q| \leq 13$ without overflow. The query diameter d_Q varied from 3 to 5, where the default value of d_Q was 3. The label size $|\Sigma_G| = 32, 64$ or 128 and the default value was 64.
- *Neighbor-label pruning* (`NL`). The value of hop h varied from 4 to 6. The default value was 4.
- *Path-based pruning* (`Path`). The value of length k for k-path varied from 3 to 5. The default value was 3.
- *Two-iteration violation pruning* (`twoIter`). We chose vertices randomly in each ball with portion p ($p = 0.1$, 0.3, or 0.5) for `twoIter`. This investigated the balance between efficiency and effectiveness of the pruning. The corresponding algorithm was denoted as $\texttt{twoIter}_p$. The default value was 0.3.
- *One-iteration violation pruning* (`oneIter`). We conducted one iteration on *all* the vertices for violation pruning.

Balls. Tab. IV shows some statistics of the balls generated from random queries under the default setting. *In a nutshell, each query can lead to several thousand balls and each ball contains hundreds of vertices.*

A. Experiment on Efficiency

EXP-0. Performance at the client. Given a query, the client generated the encrypted messages for *EncSSA* and decrypted the ciphertexts returned by the *SP* to obtain the results.

1) *Preprocessing*. Given a query Q, the *client* generated the adjacency matrix $\overline{M_Q}$, the replacement tables $\mathcal{T}_R$, the path tables $\mathcal{T}_P$ and the *NL-matrices* M_Q^h. *The total preprocessing times are all less than 0.15s.*

2) *Encryption*. The messages to be encrypted were $\overline{M_Q}$, $\mathcal{T}_R$, $\mathcal{T}_P$, M_Q^h and the chosen ciphertexts c_0 and c_1. Based on the encrypted $\overline{M_Q}$, *i.e.*, $\overline{EM_Q}$, the client generated the replacement tables $\mathcal{T}_R$ for `twoIter`. *The total encryption times are all less than 0.1s.*

3) *Decryption*. The client decrypted the messages generated from `Path`, `NL` and `twoIter`. *The total runtimes for decryption of* EncSSA *in our experiment are all less than 1s.*

4) *Message sizes*. As analyzed in Sec. IV-D, the message size is $N_{ball} \cdot (a \cdot |V_Q| + b)$, $1 \leq a, b \leq 2$, where N_{ball} is the number of computed balls. The size of each ciphertext for *CGBE* of 4096 bits is 512 bytes. Take the query for *Twitter* in the next **EXP-1** as an example. The message size is 24MB, whose transmission time is less than 0.5*s* in a 100Mbps Ethernet.

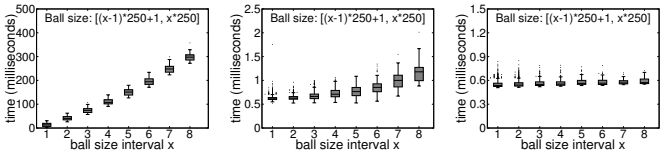

(a) $\texttt{twoIter}_{0.3}$ (186.2s) (b) `Path` (2.2s) (c) `NL` (1.6s)

Fig. 5: Runtimes of $\texttt{twoIter}_{0.3}$, `NL` and `Path` on Slashdot

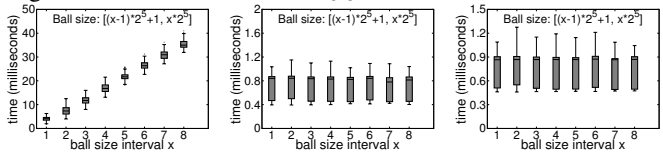

(a) $\texttt{twoIter}_{0.3}$ (58.8s) (b) `Path` (3.5s) (c) `NL` (3.2s)

Fig. 6: Runtimes of $\texttt{twoIter}_{0.3}$, `NL` and `Path` on DBLP

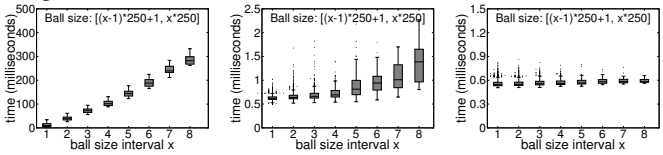

(a) $\texttt{twoIter}_{0.3}$ (220.9s) (b) `Path` (3.6s) (c) `NL` (2.6s)

Fig. 7: Runtimes of $\texttt{twoIter}_{0.3}$, `NL` and `Path` on Twitter

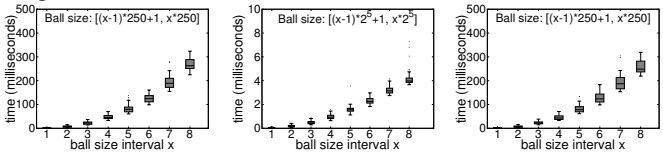

(a) Slashdot (83.5s) (b) DBLP (3.8s) (c) Twitter (83.2s)

Fig. 8: Runtimes of `Match()` on different datasets

EXP-1. Overall runtimes under the default setting. For the ease of exhibition, we used boxplots. In x-axis, we grouped the balls according to their sizes, whose definition is shown in the figures. Only 1% of balls were beyond x range. We reported the performance as *runtimes per ball*, and for brevity, we simply called them runtimes. The box of each interval was drawn around the region between the first and third quartiles, and a horizontal line at the median value. The whiskers extended from the ends of the box to the most distant point with a runtime within 1.5 times the interquartile range. Points that lie outside the whiskers were outliers. The total runtime of each technique was presented in the parentheses in the *subcaption* of each figure.

We first investigated the algorithms on the three datasets under the default setting. The results of $\textit{Slashdot}_{64}$ are presented in Fig. 5. Fig. 5(a) shows that the runtimes of $\texttt{twoIter}_{0.3}$ increase as the ball sizes $|V_B|$ increase. $\texttt{twoIter}_{0.3}$ takes roughly 300*ms* even for large balls. We remark that `oneIter` is faster than $\texttt{twoIter}_{0.5}$ but slower than $\texttt{twoIter}_{0.3}$.

As expected, `NL` is efficient and not sensitive to $|V_B|$ but the *NL-index* sizes. `Path` is also efficient but its runtimes increase as $|V_B|$ increases. This is because `Path` involved traversing the ball to check all the k-paths starting from the ball center.

The results of $\textit{DBLP}_{64}$ and $\textit{Twitter}_{64}$ are presented in Fig. 6 and Fig. 7. Similar trends can be observed with the exception of the runtimes of `Path` of $\textit{DBLP}_{64}$. The reason is that the

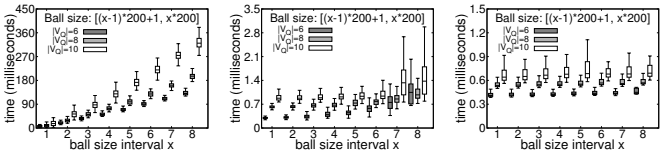

(a) $\texttt{twoIter}_{0.3}$ (b) Path (c) NL

Fig. 9: Runtimes by varying $|V_Q|$ on Slashdot

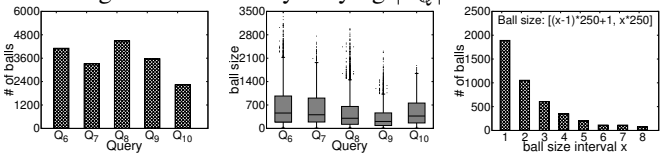

(a) # of balls (b) ball size (c) ball distribution (Q_8)

Fig. 10: Statistics of balls when varying $|V_Q|$ on Slashdot

balls of *DBLP* are very sparse, the performance differences due to the traversals for k-paths cannot be observed.

Finally, we report in Fig. 8 the runtimes of strong simulation in the *plaintext* domain to give a reference to the overhead of privacy preserving computation. We implemented Match() of [9] in our codebase. From the total runtimes indicated in the figures' subcaptions, the private algorithm is around 2.3x, 17x and 2.7x slower than Match().

EXP-2. Runtimes under different settings. We ran the algorithms on *Slashdot* and vary a parameter at a time. In the following figures, there are only fewer than 1% of outlier performances that cannot be displayed.

2.1. Varying $|V_Q|$. Fig. 9(a) shows the results for $\texttt{twoIter}_{0.3}$ on *Slashdot* for Q_6, Q_8 and Q_{10}. It can be observed that the runtime increases as either $|V_Q|$ or $|V_B|$ increases. Moreover, the trends of the runtime of $\texttt{twoIter}_{0.3}$ are slightly superlinear in practice. The runtime variations are larger when either $|V_Q|$ or $|V_B|$ becomes larger. These show $\texttt{twoIter}_{0.3}$ can always process at least 2 balls per second under various settings.

Recall that two-Iter is oblivious, where the runtime depends only on $|V_B|$ and $|V_Q|$. Hence, we further investigated $|V_B|$ and $|V_Q|$. Fig. 10(a) shows the total number of balls of different $|V_Q|$s. The number of balls for Q_6-Q_{10} ranged from 2400 to 4800. Fig. 10(b) shows the variations of $|V_B|$ and Fig. 10(c) reports that many balls have hundreds of vertices. $\texttt{twoIter}_{0.3}$ can process more than 10 such balls in 1s.

The trends of NL and Path when varying $|V_Q|$ are shown in Figs. 9(c) and 9(b). It can be observed that a larger $|V_Q|$ leads to a larger runtime. For NL, a larger query has a larger *NL-matrix*. For Path, more labels also make the path tables larger. Therefore, NL and Path become slower.

2.2. Varying p for $\texttt{twoIter}_p$. In Fig. 11, it can be observed that the runtimes of $\texttt{twoIter}_p$ increase as p increases. When p=1, the runtime of $\texttt{two-Iter}_1$ on large balls can be large. We can tune the runtime by tuning p, but introducing false positives (see Sec. VI-B).

2.3. Varying k for Path. Due to space restriction, the detailed results are presented in a technical report [21]. In a nutshell, the runtimes increase when k increases. This is because Path traverses each ball from the center to check all the k-paths. We do not observe the increase in runtimes of *DBLP* since *DBLP*

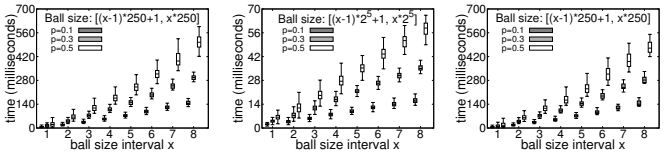

(a) *Slashdot* (b) *DBLP* (c) *Twitter*

Fig. 11: Runtimes by varying p: (0.1, 0.3 and 0.5) for twoIter

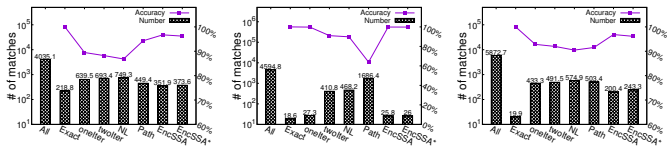

(a) *Slashdot* (b) *DBLP* (c) *Twitter*

Fig. 12: Overall accuracy and number of matches

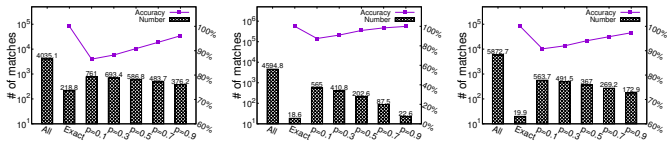

(a) *Slashdot* (b) *DBLP* (c) *Twitter*

Fig. 13: Effectiveness by varying p for $\texttt{twoIter}_p$

is sparse and the traversal times have a negligible difference.

2.4. Varying h for NL. The runtimes are generally very small and they increase as h increases [21].

B. Experiments on Effectiveness

EncSSA computes a superset of the solution of strong simulation query, in which there can be *false positives*. Thus, we investigated the accuracy of the results, defined as $(TP{+}TN)/(TP{+}TN{+}FP{+}FN)$, where TP (TN) denotes *true positive* (*true negative*), and FP (FN) denotes *false positive* (*false negative*), respectively. We remark FN=0.

We tested the effectiveness of oneIter, twoIter, NL, Path and EncSSA independently. We also tested the effectiveness of specific combinations of them on different datasets. For *Slashdot* and *Twitter*, EncSSA$*$ used twoIter, NL and Path. For *DBLP*, EncSSA$*$ used oneIter, NL and Path. All results are the average from 10 random queries.

EXP-1. Overall effectiveness under the default setting. Fig. 12 shows the number of matches obtained by each method and the corresponding accuracy. It can be observed that almost all the methods have accuracies higher than or close to 90%, with only one exception. *DBLP* is sparse and there are fewer paths with length larger than 3, which reduces the pruning power of Path. Moreover, EncSSA has the highest accuracy since its result is the intersection set of the results obtained by oneIter, twoIter, NL and Path. For EncSSA$*$, its accuracy is slightly lower than EncSSA's but its runtime is shorter than EncSSA's by turning off some specific technique(s).

EXP-2. Effectiveness under different settings. Fig. 13 shows the results when varying $p = 0.1,\ 0.3,\ 0.5,\ 0.7$ and 0.9 for $\texttt{twoIter}_p$. As expected, a larger p leads to fewer false positives but more runtimes are needed (Fig. 11). Hence, we can observe a trade-off between efficiency and effectiveness in choosing p. We further ran Path and NL. A larger k for Path leads to few false positives. The improvement from *DBLP* is

not obvious since there are few k-paths for $k \geq 4$. In NL, when $h \geq 4$, the accuracy is larger than 80%. However, it does not improve further since the center of each computed ball does not have neighbors larger than 4 hops.

VII. RELATED WORK

There have been works on privacy preserving query processing [23]–[26] in the recent three years. This section includes only graph queries and secure query framework.

Privacy preserving graph queries. Cao et al. [17] studied tree pattern queries on encrypted XML documents by predetermining the traversal order for each query. Cao et al. [18] proposed a *filtering and verification* method to solve the privacy preserving subgraph isomorphism query (*sub-iso*) over encrypted graph-structured data in cloud computing. To solve *sub-iso* in cloud computing, Fan et al. [20] transformed the classic solution into matrix operations. They studied privacy preserving *sub-iso* under two different models, *i.e.*, the structure information of both query and graph are preserved [20] and only query is preserved [16]. Chang et al. [27] also solved the privacy preserving *sub-iso* by using the *k-automorphic* graph to protect the structure information of data graphs. Gao et al. [11] studied the privacy preserving *strong simulation* query [9] in cloud. They used *k-automorphic* graph to protect the structure information of data graphs. However, the structure information of query is not preserved.

General secure query framework. Gentry et al. [13] described the first plausible construction for a fully homomorphic encryption (*FHE*) that supports both addition and multiplication operations on ciphertexts. However, due to the known poor performance, *FHE* cannot be adopted for this paper. An oblivious RAM simulator (*ORAMs*), introduced by Goldreich and Ostrovsky [28], is a compiler that transforms algorithms in such a way that the resulting algorithms preserve the input-output behavior of the original algorithm but the distribution of memory access pattern of the transformed algorithm is independent to the memory access pattern of the original algorithm. However, *ORAMs* cannot be applied in this paper since the query is not known to the *SP*. Nayak et al. [29] proposed a framework called *GraphSC* to provide a programming paradigm that allows non-cryptography experts to write secure graph-based algorithm with parallel secure oblivious implementations. Following the *Pregel/GraphLab* programming paradigm, *GraphSC* uses three primitives as interfaces, *i.e.*, *scatter*, *gather* and *apply*. However, *GraphSC* still needs the query structure for violation detection.

VIII. CONCLUSION

This paper investigates the problem of privacy preserving strong simulation queries for large graphs. This paper adopts strong simulation query as it strikes a good balance between matching flexibility and query efficiency. This paper presents an oblivious algorithm for strong simulation queries under the plaintext settings. Then, the paper proposes its encrypted version and several optimizations for an inexact efficient secure algorithm *EncSSA*. Privacy analysis results are presented. The experimental results have shown the algorithms are efficient and effective. As for future work, we plan to integrate query answer authentication into this work.

ACKNOWLEDGMENT

This work is supported by HKBU12232716 and HKBU12201518.

REFERENCES

[1] H. Tong, C. Faloutsos, B. Gallagher, and T. Eliassi-Rad, "Fast best-effort pattern matching in large attributed graphs," in *SIGKDD*, 2007.
[2] Y. Tian and J. M. Patel, "Tale: A tool for approximate large graph matching," in *ICDE*, 2008.
[3] W. Fan, "Graph pattern matching revised for social network analysis," in *ICDT*, 2012.
[4] S. A. Cook, "The complexity of theorem-proving procedures," in *STOC*, 1971.
[5] J. Kim, H. Shin, W.-S. Han, S. Hong, and H. Chafi, "Taming subgraph isomorphism for RDF query processing," *PVLDB*, 2015.
[6] P. Hell and J. Nesetril, *Graphs and Homomorphisms*, 2004.
[7] R. Milner, *Communication and Concurrency*, 1989.
[8] S. Mennicke, J.-C. Kalo, D. Nagel, H. Kroll, and W.-T. Balke, "Fast dual simulation processing of graph database queries," in *ICDE*, 2019.
[9] S. Ma, Y. Cao, W. Fan, J. Huai, and T. Wo, "Strong simulation: Capturing topology in graph pattern matching," *TODS*, 2014.
[10] B. W. Hung and A. P. Jayasumana, "Investigative simulation: Towards utilizing graph pattern matching for investigative search," in *ASONAM*, 2016, pp. 825–832.
[11] J. Gao, J. Xu, G. Liu, W. Chen, H. Yin, and L. Zhao, "A Privacy-Preserving Framework for Subgraph Pattern Matching in Cloud," in *DASFAA*, 2018.
[12] D. Eppstein, M. T. Goodrich, and R. Tamassia, "Privacy-preserving data-oblivious geometric algorithms for geographic data," in *SIGSPATIAL*, 2010.
[13] C. Gentry and D. Boneh, *A Fully Homomorphic Encryption Scheme*, 2009.
[14] Y. Lindell and J. Katz, *Introduction to Modern Cryptography*, 2014.
[15] D. Boneh, E.-J. Goh, and K. Nissim, "Evaluating 2-DNF formulas on ciphertexts," in *TCC*, 2005.
[16] Z. Fan, B. Choi, J. Xu, and S. S. Bhowmick, "Asymmetric structure-preserving subgraph queries for large graphs," in *ICDE*, 2015.
[17] J. Cao, F.-Y. Rao, M. Kuzu, E. Bertino, and M. Kantarcioglu, "Efficient tree pattern queries on encrypted xml documents," in *EDBT/ICDT*, 2013.
[18] N. Cao, Z. Yang, C. Wang, K. Ren, and W. Lou, "Privacy-preserving query over encrypted graph-structured data in cloud computing," in *ICDCS*, 2011.
[19] H. Hu, J. Xu, Q. Chen, and Z. Yang, "Authenticating location-based services without compromising location privacy," in *SIGMOD*, 2012.
[20] Z. Fan, B. Choi, Q. Chen, J. Xu, H. Hu, and S. S. Bhowmick, "Structure-preserving subgraph query services," *TKDE*, 2015.
[21] L. Xu, J. Jiang, B. Choi, J. Xu, and S. S. Bhowmick, "Privacy preserving pattern query processing for large graphs," *https://www.comp.hkbu.edu.hk/%7Ecslyuxu/lyu2020tr.pdf*, 2020.
[22] J. Leskovec and A. Krevl, "SNAP," http://snap.stanford.edu/data.
[23] J. Bater, Y. Park, X. He, X. Wang, and J. Rogers, "Saqe: practical privacy-preserving approximate query processing for data federations," *PVLDB*, 2020.
[24] S. Wu, Q. Li, G. Li, D. Yuan, X. Yuan, and C. Wang, "Servedb: Secure, verifiable, and efficient range queries on outsourced database," in *ICDE*, 2019.
[25] X. Lei, A. X. Liu, R. Li, and G.-H. Tu, "Seceqp: A secure and efficient scheme for sknn query problem over encrypted geodata on cloud," in *ICDE*, 2019.
[26] N. Cui, X. Yang, B. Wang, J. Li, and G. Wang, "Svknn: Efficient secure and verifiable k-nearest neighbor query on the cloud platform," in *ICDE*, 2020.
[27] Z. Chang, L. Zou, and F. Li, "Privacy preserving subgraph matching on large graphs in cloud," in *SIGMOD*, 2016.
[28] O. Goldreich and R. Ostrovsky, "Software protection and simulation on oblivious rams," *JACM*, 1996.
[29] K. Nayak, X. S. Wang, S. Ioannidis, U. Weinsberg, N. Taft, and E. Shi, "Graphsc: Parallel secure computation made easy," in *S&P*, 2015.